AlGaN/GaN MIS-HEMT using NbAlO dielectric layer grown by atomic layer deposition*

Bi Zhi-Wei(毕志伟)[a)†], Feng Qian(冯 倩)[a)], Hao Yue(郝 跃)[a)‡], Wang Dang-Hui(王党会)[b)], Ma Xiao-Hua(马晓华)[a)], Zhang Jin-Cheng(张进成)[a)], Quan Si(全 思)[a)], and Xu Sheng-Rui(许晟瑞)[a)]

[a)] *Key Laboratory of Wide Band-Gap Semiconductor Materials and Devices, The School of Microelectronics, Xidian University, Xi'an* 710071, *China*

[b)] *School of Materials Science and Engineering, Xi'an Shiyou University, Xi'an* 710065, *China*

(Received 23 November 2009; revised manuscript received 16 January 2010)

We present an AlGaN/GaN metal–insulator–semiconductor high electron mobility transistor (MIS-HEMT) with an NbAlO high-k dielectric deposited by atomic layer deposition (ALD). Surface morphology of samples are observed by atomic force microscopy (AFM), indicating that the ALD NbAlO has an excellent-property surface. Moreover, the sharp transition from depletion to accumulation in capacitance–voltage (C–V)curse of MIS-HEMT demonstrates the high quality bulk and interface properties of NbAlO on AlGaN. The fabricated MIS-HEMT with a gate length of 0.5 μm exhibits a maximum drain current of 960 mA/mm, and the reverse gate leakage current is almost 3 orders of magnitude lower than that of reference HEMT. Based on the improved direct-current operation, the NbAlO can be considered to be a potential gate oxide comparable to other dielectric insulators.

Keywords: AlGaN/GaN, MIS-HEMT, NbAlO, high-k
PACC: 7340J, 7340N

1. Introduction

Wide bandgap AlGaN/GaN high-electron mobility transistors (HEMTs) are emerging as excellent candidates for radio-frequency (RF) and microwave power amplifiers because of their high-power-handling capabilities. The recent progress in the development of AlGaN/GaN high electron mobility transistors (HEMTs) for high-frequency and high-power applications has been very rapid.[1,2] However, it has been observed that the Schottky gate of HEMT tends to degrade with gate leakage current increasing, especially when the HEMT operates in the high power condition. Therefore, different gate insulation layers have been used as one of the possible solutions to deal with the gate leakage problems by increasing the energy barrier. On the other hand, some dielectrics dielectric materials that can be used as passivating layers, may significantly reduce the degree of current collapse by preventing strain in the GaN barrier from being induced by the applied gate bias.[3]

In the previous studies, SiO_2,[4] Al_2O_3,[5,6], Si_3N_4,[7] HfO_2[8] have all been used as the insulating materials of MIS-HEMTs, Kordos *et al.* pointed out that the interface between $Al_2O_3$and AlGaN was better than between SiO_2 and Si_3N_4, therefore, Al_2O_3 have a better passivation effect such that the transconductance of Al_2O_3 MOS-HEMT can be improved obviously.[5,9]

Although the permittivity of Al_2O_3 is 8.9, it is still a lower value for gate dielectric The use of of high-k dielectric could conduce to solving many problems, because larger dielectric constant could translate to more efficient gate modulation, therefore, some high-k dielectrics dielectric materials such as HfO_2 ($k \sim 45 - 150$) are being used as gate dielectric in order to eliminate these drawbacks.[8] However, HfO_2 hardly has the good interface with the AlGaN layer, furthermore, the crystal temperature of HfO_2 is only 375°, and these defects restrict the application of some binary dielectric materials to GaN.

In this paper, we present AlGaN/GaN MIS-HEMTs with NbAlO dielectric for the gate insulation and surface passivation NbAlO can be prepared

*Project supported by the State Key Program and Major Program of National Natural Science Foundation of China (Grant Nos. 60736033 and 60890191).
†E-mail: zhwbi@126.com
‡Corresponding author. E-mail: yhao@xidian.edu.cn
© 2010 Chinese Physical Society and IOP Publishing Ltd

in such a way that Nb is mixed into Al_2O_3. The adulteration of Nb can improve the permittivity obviously and the NbAlO has a good temperature characteristic. We show that the reverse gate leakage current is reduced substantially, and the maximum saturation current is enhanced apparently, moreover, we observe an increase in GVS, which is defined as a 10% drop of $g_{\mathrm{M.MAX}}$.

2. Experiment

The AlGaN/GaN material structure used in this study was composed of a 40 nm LT-GaN nuclear layer, a 2380nm unintentionally doped GaN layer, a 1.5-nm AlN insert layer, and a 22-nm $Al_{0.3}Ga_{0.7}N$ barrier layer on a 2-inch c-plane sapphire substrate. The room-temperature Hall mobility and the sheet carrier concentration were 1544 $cm^2/(V{\cdot}s)$ and $1.2{\times}10^{13}$ cm^3, respectively. Detailed surface morphologies of samples were characterized by the atomic force microscopy(AFM)with using an Agilent 5500 scanning probe system.

For the MIS structure, an additional 2.6-nm Al_2O_3 /9.6-nm NbAlO laminated layer was then sequentially deposited on half of the sample by atomic layer deposition (ALD). Figure 1 shows the surface morphologies of samples before and after ALD dielectric layer separately. From the surface of the AlGaN sample can be found a lot of defects and pits, which can act as leakage paths as shown in Fig. 1(a). In contrast, after ALD dielectric layer few defects and pits are observed, the surface of NbAlO is more smooth, and the root mean square (rms)of NbAlO is much smaller than that of AlGaN, all of these show that ALD NbAlO has an excellent-property surface.

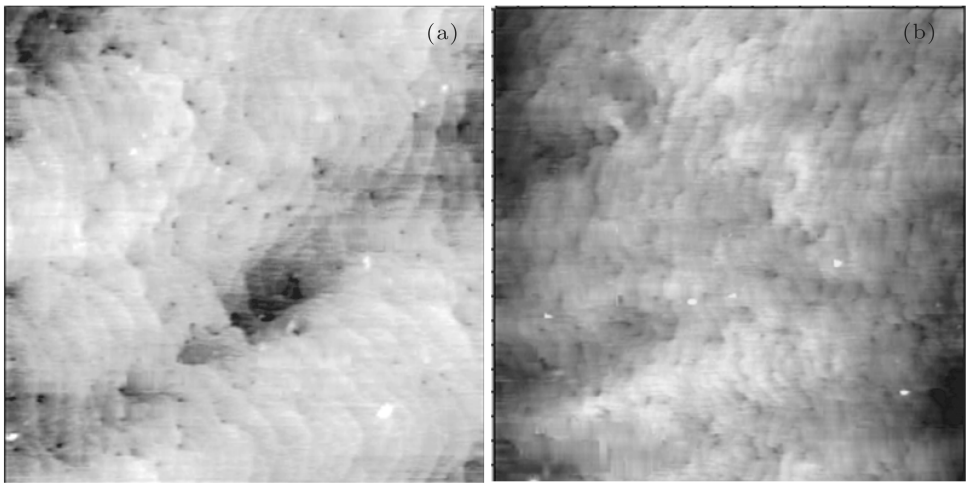


Fig. 1. Typical $5{\times}5$ μm^2 AFM scans showing the surface morphology of AlGaN (a) and NbAlO (b).

In order to form Ohmic contact, the high-k dielectric layer above the Ohmic contact area was removed by reactive ion etch (RIE) etching. The Ti/Al/Ni/Au multilayer metal was deposited by e-beam evaporation and patterned as Ohmic contacts on the exposed AlGaN barrier. The mesa isolation process with BCl_3 plasma RIE was used for device isolation. Using Ni/Au for the gate electrode fabrication, two kinds of devices were fabricated on the same wafer. The gate length and the gate width on the fabricated device are 0.5 and 100 μm, respectively. The device dc electrical characteristics were measured at room temperature by using an Angilent 1500 semiconductor parameter analyzer.

3. Results and discussion

Figure 2 shows the capacitance–voltage (C–V) characteristics measured at 1 MHz on gate capacitors of both the MIS-HEMT and the HEMT structures. The sharp transition from depletion to accumulation in capacitance–voltage (C–V)curse of MIS-HEMT is similar to that of the HEMT and demonstrates the

highquality bulk and interface properties of NbAlO on AlGaN. From the capacitance of HEMT, and using AlGaN layer permittivity $\varepsilon_{\rm B} = 8.8$ and capacitor area $S = \pi \times 65 \times 65$ (μm^2), we can estimate the thickness of AlGaN barrier ($d_{\rm B}$) to be 20.25 nm. The thickness of the dielectric layer ($d_{\rm OX}$) can be extracted from the measured pad capacitances

$$C_{\rm MOS} = \frac{\varepsilon_0\varepsilon_{\rm B}}{d_{\rm B}} \times \left(1 + \frac{d_{\rm OX}}{d_{\rm B}} \cdot \frac{\varepsilon_{\rm B}}{\varepsilon_{\rm OX}}\right)^{-1} = C_{\rm MS} \times \left(1 + \frac{d_{\rm OX}}{d_{\rm B}} \cdot \frac{\varepsilon_{\rm B}}{\varepsilon_{\rm OX}}\right)^{-1}, \quad (1)$$

where $C_{\rm MOS}$ and $C_{\rm MS}$ are the capacitances of MIS-HEMT and the HEMT, $\varepsilon_{\rm OX} = 15$ is the average permittivity of dielectric. Using the data of Fig. 2, the dielectric layer $d_{\rm OX}$ was estimated to be 15nm, this value is larger than the design value of 12.2 nm, that is probably due to the doping concentration of Nb lower than design value in the progress of ALD NbAlO, which leadd to a lower value of $\varepsilon_{\rm OX}$.

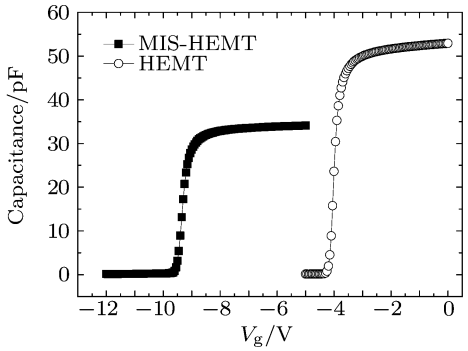


Fig. 2. Measured C–V characteristics of MIS-HEMT and HEMT.

Figures 3 and 4 show the dc I–V curves of HEMT and MIS-HEMT at room temperature The gate voltage varies from −10 V to +2 V for the MIS-HEMT. The maximum drain current density of MIS-HEMT measured at gate bias of +2 V is approximately 960 mA/mm, and this value is higher than 800 mA/mm for the HEMT. A similar result is observed by Stoklas *et al.*, they fabricated AlGaN/GaN MIS-HEMT by using thin Al_2O_3 dielectric.[10] This result can be attributed to the increase in sheet carrier concentration in the channel with Al_2O_3 /NbAlO dielectric. An effective passivation of traps at the AlGaN surface, which reduces the surface-related depletion of the channel layer and increases the sheet electron density in the 2D channel, can be obtained by using Al_2O_3 layers.[11]

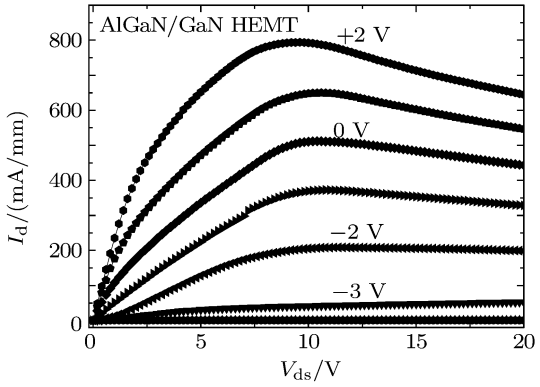


Fig. 3. I–V characteristics of AlGaN/GaN HEMT.

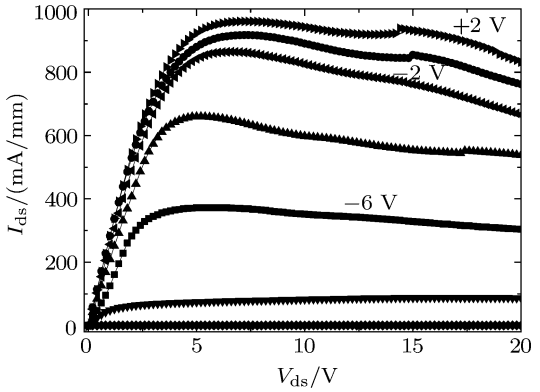


Fig. 4. I–V characteristics of AlGaN/GaN MIS-HEMT.

The typical threshold voltages for MIS-HEMT and HEMT are 78 V and −3.6 V, respectively. The increase of pinch-off voltage of MIS-HEMT is due to the larger separation of 2DEG from metal by NbAlO dielectric.

Figures 5 and 6, respectively, show the comparisons of the transfer and the transconductance characteristic between AlGaN/GaN MIS-HEMT and HEMT fabricated on the same wafer, and the drain-to-source voltage is 10 V. From Fig. 5, we can find the drain current densities of MIS-HEMT and HEMT to be 979 and 768 mA/mm with the same gate bias of +2 V, respectively. The output current increases 27% for the MIS-HEMT compared with that for the HEMT. The increase of output current reveals that the NbAlO high-k dielectric effectively can passivate the surface of AlGaN and reduce the surface states due to the high quality of ALD NbAlO. The combination of higher breakdown voltage and higher drain current indicates the superiority of MIS-HEMT for high-performance power amplifier applications.

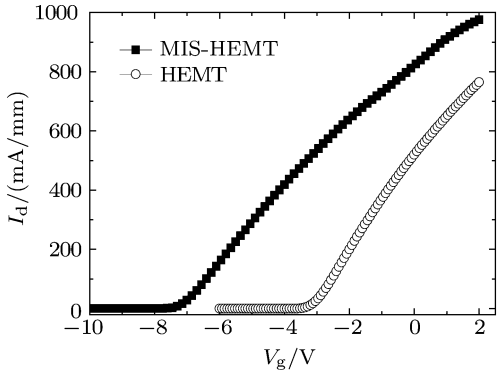


Fig. 5. Transfer characteristics for the MIS-HEMT and HEMT with a drain-to-source voltage of 10 V.

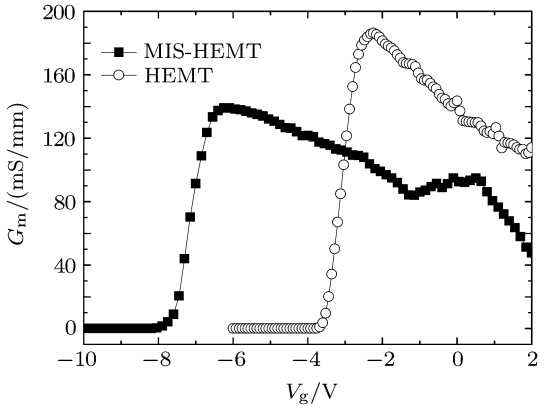


Fig. 6. Transconductance characteristics measured for the MIS-HEMT and HEMT with a drain-to-source voltage of 10 V.

The maximum values of transconductance (g_{MMAX}) for MIS-HMET and conventional HEMT are 140 and 186 mS/mm respectively. Although we used NbAlO high-k dielectric as the gate insulator, a drop of 24% in the transconductance value of MIS-HMET compared with that of HEMT can be found to be same for all cases, and the reduction is expected from the larger source resistance due to large transfer resistance with the increase of separation of the 2DEG from the Schottky gate metal.[12] However a reduction of 46mS/mm is a lower value than that of 12 nm SiO_2 MOS-HEMT, which was fabricated by Kordos *et al.*[4] and the reduction of transconductance is 65 mS/mm, this improvement profits from the using of high-k dielectric.

Figure 7 shows the forward and reverse gate currents for the MIS-HEMT and the HEMT, separately. The curves clearly reveal that the MIS-HEMT reverse gate leakage current is almost three orders of magnitude smaller than that for the conventional HEMT. This value is also comparable to those of other MIS-HEMTs with using other dielectric materials such as Al_2O_3,[13] the forward gate leakage is similar to that of the HEMT, this phenomenon can be explained by F–N Tunneling.[14] For high-power microwave applications, the gate–drain diodes often operate in the condition of reverse-bias, therefore, the better reverse gate leakage can increase the breakdown voltage and improve reliability obviously

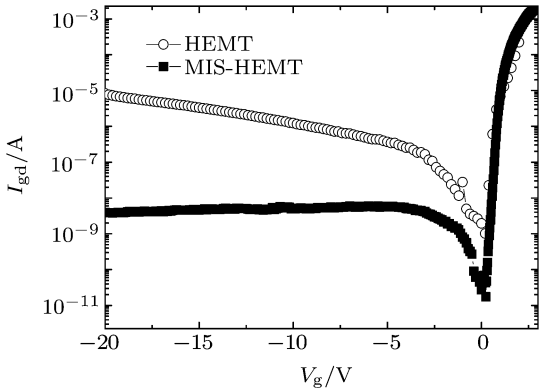


Fig. 7. Gate leakages of gate–drain diode for the MIS-HEMT and HEMT on the substrates with the same structures.

4. Conclusions

ALD NbAlO is proved to be an excellent gate dielectric for AlGaN/GaN MIS-HEMT, the 0.5 μm gate length MIS-HEMT with an Al_2O_3/NbAlO oxide thickness of 12.2 nm is fabricated, which exhibits a maximum transconductance of 140 mS/mm and an enhanced maximum drain current of 960 mA/mm, in addition, the reverse gate leakage current was at least 3 orders of magnitude lower than that of reference HEMT with the same structure of substrate, all of these advantages show that the NbAlO is a viable alternative to regular HMET for high-power, high-frequency, high-temperature applications.

References

[1] Kumar V, Lu W, Schwindt R and Kuliev A 2002 *IEEE Electron Device Lett.* **23** 455

[2] Barker J M, Ferry D K and Koleske D D 2005 *J. Appl. Phys.* **97** 63705-1

[3] Yue Y Z, Hao Y, Zhang J C, Feng Q, Ni J Y and Ma X H 2008 *Chin. Phys.* B **17** 1405

[4] Kordos P, Heidelberger G, Bernat J, Fox A, Marso M and Luth H 2005 *Appl. Phys. Lett.* **87** 143501

[5] Kordos P, Gregusova D, Stoklas R, Gazi S and Novak J 2008 *Solid State Electronics* **52** 973

[6] Feng Q, Tian Y, Bi Z W, Yue Y Z, Ni J Y, Zhang J C, Hao Y and Yang L A 2009 *Chin. Phys.* B **18** 3014

[7] Wang R N, Cai Y, Tang C W, Lau K M and Che K J 2006 *IEEE Electron Device Lett.* **27** 793

[8] Liu C, Chor E F and Tan L S 2006 *Appl. Phys. Lett.* **88** 173504

[9] Bi Z W, Feng Q, Hao Y, Yue Y Z, Zhang Z F, Mao W, Yang L Y and Hu G Z 2009 *Acta Phys. Sin.* **58** 7211 (in Chinese)

[10] Stoklas R, Gregusova D, Novak J, Vescan A and Kordos P 2008 *Appl. Phys. Lett.* **93** 124103

[11] Okino T, Ochiai M, Ohno Y, Kishimoto S, Maezava K and Mizutine T 2004 *IEEE Electron Device Lett.* **25** 523

[12] Ye P D, Yang B, Ng K K and Bude J 2005 *Appl. Phys. Lett.* **86** 063501

[13] Yue Y Z, Hao Y, Feng Q, Zhang J C, Ma X H and Ni J Y 2007 *Chin. Phys. Lett.* **24** 2419

[14] Feng Q, Hao Y and Yue Y Z 2008 *Acta Phys. Sin.* **57** 1886 (in Chinese)